Diabetologia (2018) 61:2621–2632
https://doi.org/10.1007/s00125-018-4730-z

ARTICLE

Silencing of high-affinity insulin-reactive B lymphocytes by anergy and impact of the NOD genetic background in mice

Mia J. Smith[1,2] · Rochelle M. Hinman[1] · Andrew Getahun[1] · Soojin Kim[1] · Thomas A. Packard[1] · John C. Cambier[1]

Received: 21 March 2018 / Accepted: 16 August 2018 / Published online: 25 September 2018

Abstract

Aims/hypothesis Previous studies have demonstrated that high-affinity insulin-binding B cells (IBCs) silenced by anergy in healthy humans lose their anergy in islet autoantibody-positive individuals with recent-onset type 1 diabetes, and in autoantibody-negative first-degree relatives carrying certain risk alleles. Here we explore the hypothesis that IBCs are found in the immune periphery of disease-resistant C57BL/6-H2g7 mice, where, as in healthy humans, they are anergic, but that in disease-prone genetic backgrounds (NOD) they become activated and migrate to the pancreas and pancreatic lymph nodes, where they participate in the development of type 1 diabetes.

Methods We compared the status of high-affinity IBCs in disease-resistant VH125.C57BL/6-H2g7 and disease-prone VH125.NOD mice.

Results Consistent with findings in healthy humans, high-affinity IBCs reach the periphery in disease-resistant mice and are anergic, as indicated by a reduced expression of membrane IgM, unresponsiveness to antigen and failure to become activated or accumulate in the pancreatic lymph nodes or pancreas. In NOD mice, high-affinity IBCs reach the periphery early in life and increase in number prior to the onset of hyperglycaemia. These cells are not anergic; they become activated, produce autoantibodies and accumulate in the pancreas and pancreatic lymph nodes prior to disease development.

Conclusions/interpretation These findings are consistent with genetic determination of the escape of high-affinity IBCs from anergy and their early contribution to the development of type 1 diabetes.

Keywords Anergy · Autoantibodies · Autoimmunity · B cell · Diabetes · Insulin · NOD

Abbreviations

BCR	B cell receptor
IBC	Insulin-binding B cell
MACS	Magnetic-activated cell sorting
MFI	Mean fluorescence intensity
mIgM	Membrane IgM
pLN	Pancreatic lymph node
PTEN	Phosphatase and tensin homologue
Syk	Spleen tyrosine kinase

Mia J. Smith and Rochelle M. Hinman contributed equally to this study.

✉ John C. Cambier
John.Cambier@ucdenver.edu

[1] Department of Immunology and Microbiology, University of Colorado School of Medicine, P18-8100, RC1 North, 12800 East 19th Avenue, Aurora, CO 80045-2537, USA

[2] Department of Microbiology, Immunology, and Pathology, Colorado State University, Fort Collins, CO, USA

Introduction

Although T cells are the primary pathogenic effectors in type 1 diabetes, mounting evidence indicates that B lymphocytes play an essential role in disease development [1–5]. The mechanism by which B cells contribute to type 1 diabetes remains elusive, but B cell receptor (BCR) antigen specificity for islet autoantigen has been shown to be essential [6, 7]. Interestingly, although anti-islet antibodies may play a role [8], they are not required for disease development [9]. Studies in the NOD mouse model of diabetes indicate that B cells are necessary for islet antigen presentation to both CD4 and CD8 T cells [10, 11].

The action of islet antigen-reactive B cells in type 1 diabetes presumably requires a breach in tolerance mechanisms: receptor editing, clonal deletion and/or anergy. Recent studies in humans have demonstrated that high-affinity autoreactive B cells reside in the anergic compartment in healthy individuals. However, early in the development of type 1 diabetes, autoimmune thyroid

Research in context

What is already known about this subject?

- Insulin-binding B cells (IBCs) are required for the development of diabetes in NOD mice, yet previous studies indicate that IBCs in NOD mice are anergic
- In healthy humans, high-affinity IBCs are restricted to the anergic peripheral blood B cell compartment, but in autoantibody-positive individuals with recent-onset type 1 diabetes, and first-degree relatives carrying certain risk alleles, these cells leave the B cell compartment, suggesting loss of tolerance

What is the key question?

- Does the role of high-affinity IBCs in the development of type 1 diabetes in the NOD mouse emulate their hypothetical role in the development of disease in humans?

What are the new findings?

- Peripheral high-affinity IBCs are anergic in disease-resistant mice, but in disease-susceptible mice these cells become activated, produce autoantibodies and accumulate in the pancreas and pancreatic lymph nodes prior to disease development

How might this impact on clinical practice in the foreseeable future?

- Understanding how IBCs participate in the pathogenesis of type 1 diabetes may provide a rationale for targeting these cells in the clinic to prevent or treat type 1 diabetes. It may also provide essential tools for evaluating the efficacy and mode of action of candidate antigen-specific therapies

disease and systemic lupus erythematosus, autoantigen-reactive anergic B cells leave this compartment [12–14] and become activated [13], accumulating in the target organs (M. J. Smith and J. C. Cambier, unpublished observations). Owing to the difficulty of tracking these cells and monitoring their function and participation in development of disease in humans, exploration in animal models, such as the NOD mouse, is critical.

Fixation of the B cell repertoire by immunoglobulin transgenesis has allowed the study of B cell tolerance to autoantigens, such as insulin in the Tg125 anti-insulin transgenic mouse [6]. It has been reported that in both disease-sensitive Tg125.NOD and disease-resistant Tg125.C57BL/6 mice, B cells mature normally yet are anergic based on a failure to proliferate or on an impairment of calcium flux following stimulation [15, 16]. However, unlike in other anergy models, these 'anergic' autoreactive B cells respond to BCR stimulation by upregulation of CD86, and phosphorylation of spleen tyrosine kinase (Syk) and phosphoinositide phospholipase C γ, and can act as antigen-presenting cells to T cells, findings inconsistent with an anergic status [15, 17–20]. Thus the available evidence paints a muddled picture. Although mice that lack insulin-binding B cells (IBCs) have a greatly decreased incidence of disease [6], the reportedly anergic IBCs in Tg125.NOD mice support the development of diabetes at a rate similar to that seen in NOD mice [15]. Moreover, previous studies have reported that Tg125 mice with a C57BL/6 background do not develop disease, possibly owing to IBC anergy. However, wild-type B cells on a C57BL/6 background do not carry the necessary MHCII allotype (H2g7) to support the presentation of insulin to T cells [11]. Given that Tg125 B cells on a C57BL/6 background also do not carry the necessary MHC allotype, their use as a model of type 1 diabetes development is limited. Finally, in Tg125 mice IBCs are not starved by normal competition for survival factors, decreasing their relevance as a model for B cell tolerance.

This study explores these questions using a more physiological model in which 1–2% of B cells are insulin reactive by virtue of transgenic expression of the VH125 heavy chain [21, 22]. This heavy chain pairs with endogenous immunoglobulin light chains to achieve repertoire diversity [6]. Results demonstrate that in diabetes-susceptible (VH125.NOD) and resistant mice carrying the same MHCII allotype (VH125.C57BL/6-H2g7), B cells with BCR affinity sufficiently high to sense insulin at physiological concentrations [23] are phenotypically and functionally distinct. Our results provide insight into the participation of high-affinity IBCs in type 1 diabetes.

Methods

Mice Mice expressing the IgM^a heavy chain insulin-binding transgenes VH125 [Cg-Tg(Igh-6/Igh-V125)2Jwt/JwtJ] or non-insulin binding VH281 [Tg(Igh-6/Igh-V281)3Jwt/JwtJ] on NOD and C57BL/6 backgrounds were kindly supplied by J. W. Thomas (Vanderbilt University, TN, USA) [6, 15]. Mice expressing the IgM heavy chain VH281 were used as a control strain in this study since they differ from VH125 mice in that they lack IBCs in the periphery [6]. VH125.C57BL/6 mice

were crossed with C57BL/6-H2g7 [B6.NOD-(D17Mit21-D17Mit10)/LtJ] (Jackson Labs, Bar Harbor, ME, USA) to create VH125.C57BL/6-H2g7 mice, which carry the same MHCII as NOD mice. Unless otherwise indicated, 8- to 12-week-old non-diabetic female mice were used for all experiments. Two consecutive blood glucose readings of over 13.88 mmol/l (OneTouch Ultramini meter, OneTouch, Wayne, PA, USA) identified the mice as diabetic. Diabetic mice were humanely euthanised. Animals were housed at National Jewish Health (Denver, CO, USA) or University of Colorado School of Medicine (Aurora, CO, USA) under specific pathogen-free conditions. Experimentation was approved by the respective Institutional Animal Care and Use committees.

Tissue processing for single-cell suspensions Splenocytes were prepared and erythrocytes lysed using ammonium-chloride-potassium lysing buffer (prepared in the Cambier lab). Pancreatic lymphocytes were isolated, as previously described [24, 25]. Briefly, the pancreases were cut into small pieces and incubated in collagenase solution for 15 min at 37°C. Cells were pipetted up and down to break up the remaining tissues, and the cells were then suspended in magnetic-activated cell sorting (MACS) buffer (Miltenyi, San Diego, CA, USA), vortexed and allowed to settle for 1 min. The suspended cells were filtered and spun down. The cell pellet was resuspended in enzyme-free cell dissociation buffer (Gibco, Waltham, MA, USA). The cells were rested at room temperature for 10 min and then spun down and stained for flow cytometric analysis.

Identification and enrichment of B cells based on BCR binding to insulin As previously described [12, 26], cells were stained at 4°C with 0.1 μg insulin–biotin per 10^6 cells per 100 μl and antibodies (as described below) for 30 min, fixed with 2% (wt/vol.) formaldehyde and incubated with streptavidin–Alexa^{647} (Thermo Fisher Scientific, Waltham, MA, USA) for 15 min. Cells were then washed and incubated with anti-Cy5/anti-Alexa^{647} microbeads (Miltenyi) for 10 min and passed over magnetised LS columns (Miltenyi). Columns were washed three times, and bound cells were eluted in 6 ml of MACS buffer.

Flow cytometry analysis Cells were stained with antibodies directed against the following molecules: B220 (BD, San Jose, CA; RA3-6B2), CD19 (BioLegend, San Diego, CA, USA; 6D5), CD21/35 (BioLegend; 7E9), CD23 (BioLegend; B3B4), CD24 (BioLegend; M1/69), CD86 (BD; GL-1), CD69 (BD; H1.2F3), CD138 (BioLegend; 281-2), λ light chains (SouthernBiotech, Birmingham, AL, USA; 1060) and IgM (Cambier lab, Aurora, CO, USA; b-7-6). Dilutions were based on the manufacturers' instructions, and specificity was verified using T cells as a negative control for B cell markers, and macrophages as a positive control for the activation marker CD86. Fluorescence minus one samples were used for compensation. Flow cytometry was performed on an LSRFortessa X-20 (BD) and data analysed with FlowJo software version 8.8 (Ashland, OR, USA).

Analysis of intracellular free calcium Splenocytes (10^7 cells/ml) were incubated in 37°C RPMI, 2% (wt/wt) BSA and 1 μmol/l Indo-1, AM (Molecular Probes, Eugene, OR, USA) for 30 min. Anti-CD19, Fab anti-IgM and biotinylated insulin were added during Indo loading. Insulin binding was detected by staining with DyLight 650 (Thermo Fisher Scientific) Fab anti-biotin for 15 min. Fab fragments were used to avoid cell stimulation. Cells (2×10^6/0.4 ml) were analysed using an LSR Fortessa X-20 flow cytometer to establish a baseline, and then stimulated with 5 μg F(ab′)$_2$ goat anti-mouse IgM (Jackson Labs).

PhosFlow Syk and PTEN analysis Splenocytes (10^7 cells/ml) were stimulated with 5 μg/ml goat anti-mouse IgM (Jackson Labs) for 5 min at 37°C, or left unstimulated. Cells were immediately fixed with 2% paraformaldehyde (wt/vol.) at 37°C for 10 min, pelleted and resuspended in 100% methanol at −80°C and placed on ice for 30 min. Cells were stained with biotinylated insulin and antibodies against CD19 (BD), IgM (BD), ζ-chain-associated protein kinase 70 (ZAP70)/Syk (BD), PTEN (phosphatase and tensin homologue; BD) or isotype control (BD). Cells were washed and stained with streptavidin–Alexa^{421} (Thermo Fisher Scientific) secondary to identify IBCs.

Anti-insulin ELISA microtitre plates (Costar, Corning, NY, USA) were coated with 10 μg/ml recombinant human insulin (Sigma-Aldrich, St Louis, MO, USA) in PBS overnight at 4°C, followed by incubation with blocking buffer solution (3% BSA [wt/wt]) for 1.5 h at room temperature. Sera from 8- to 10-week-old female mice were serially diluted in blocking buffer and incubated in 96-well plates for 2 h at room temperature. Between all steps the plates were washed four times with PBS containing 0.05% (wt/vol.) Tween-20 (Sigma-Aldrich). Horseradish peroxidase goat anti-mouse IgM (Jackson Labs) followed by development with 3,3′,5,5′-tetramethylbenzidine (TMB) (Invitrogen, Waltham, MA, USA) was used to detect antibody binding. Reactions were stopped using 1000 mmol/l H_2PO_4 (Sigma-Aldrich). Antibody was measured based at an absorbance of 450 nm using a VERSAMax plate reader (Molecular Devices, San Jose, CA, USA), and data were analysed with SoftMax Pro software (Molecular Devices; https://www.moleculardevices.com/products/microplate-readers/acquisition-and-analysis-software/softmax-pro-software).

Statistics Data were analysed using Prism software version 7.0 (GraphPad Software, La Jolla, CA, USA). The logrank (Mantel–Cox) method was used to compare disease curves throughout. An unpaired Student's *t* test was used to compare

differences between groups for Figs 1, 2 and 3. Mann–Whitney *U* tests were used to compare differences between groups for Figs 4 and 5. ANOVA was used to analyse data means with repeated measures when appropriate. Data are expressed as means (SEM). A p value of <0.05 was considered significant. Randomisation and blinding was not carried out. No animals or data were excluded from these experiments.

Results

Identification and isolation of IBCs Experiments were made possible by the development of methodology to identify and enrich B cells that bind insulin via their BCRs [12, 26]. Figure 1a shows a representative diagram of the enrichment scheme, and demonstration of the specificity of the reaction, by competitive inhibition of the binding of biotinylated insulin with excess unlabelled insulin. Using this method, we found that IBCs from VH125.C57BL/6-H2g7 mice bound significantly less antigen than IBCs from VH125.NOD mice based on staining intensity (mean fluorescence intensity [MFI]), whether we compared magnetic particle enriched or unenriched populations (Fig. 1b, c). This result is consistent with the possibility that IBCs in VH125.C57BL/6-H2g7 mice have downregulated membrane IgM (mIgM) receptors, consistent with anergy [27, 28].

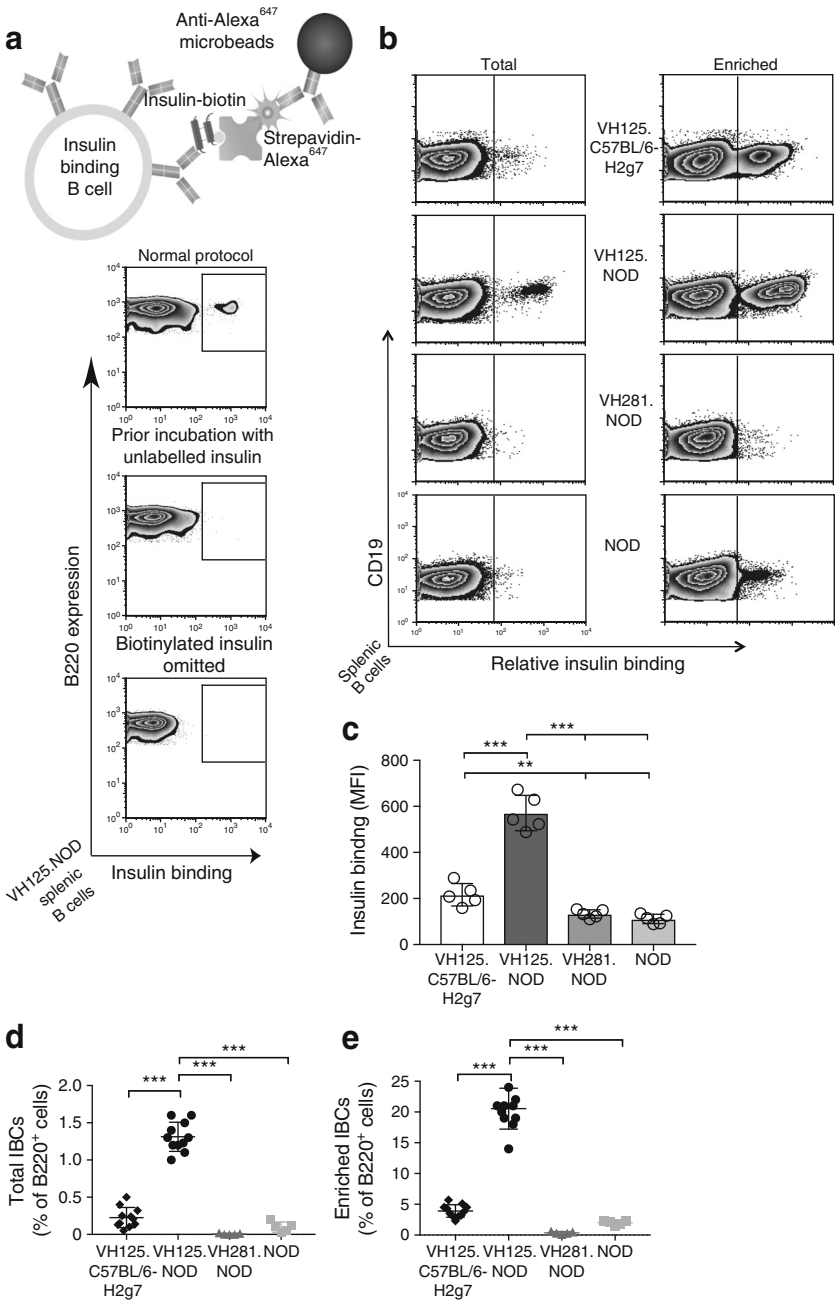

Fig. 1 Detection and enrichment of IBCs in disease-resistant and disease-prone mice. (**a**) Diagram of the absorbent used for the magnetic-particle-based staining and enrichment of IBCs. Splenic cells from VH125.NOD mice were subjected to the enrichment protocol in the presence of 50× unlabelled insulin, or in the absence of biotinylated insulin. (**b**) Representative cytograms comparing the total and enriched populations of splenic IBCs from female 8- to 12-week-old VH125.C57BL/6-H2g7, VH125.NOD, VH281.NOD and NOD mice. (**c**) MFI of IBCs compared across the four strains ($n = 5$ for each group). (**d**, **e**) Total (**d**) and enriched (**e**) splenic IBCs as a percentage of $B220^+$ B cells in the various mouse strains ($n =$ 10 for each group). Results are representative of at least three replicate experiments and are expressed as mean ± SEM. $^{**}p < 0.01$, $^{***}p < 0.001$, unpaired Student's t test

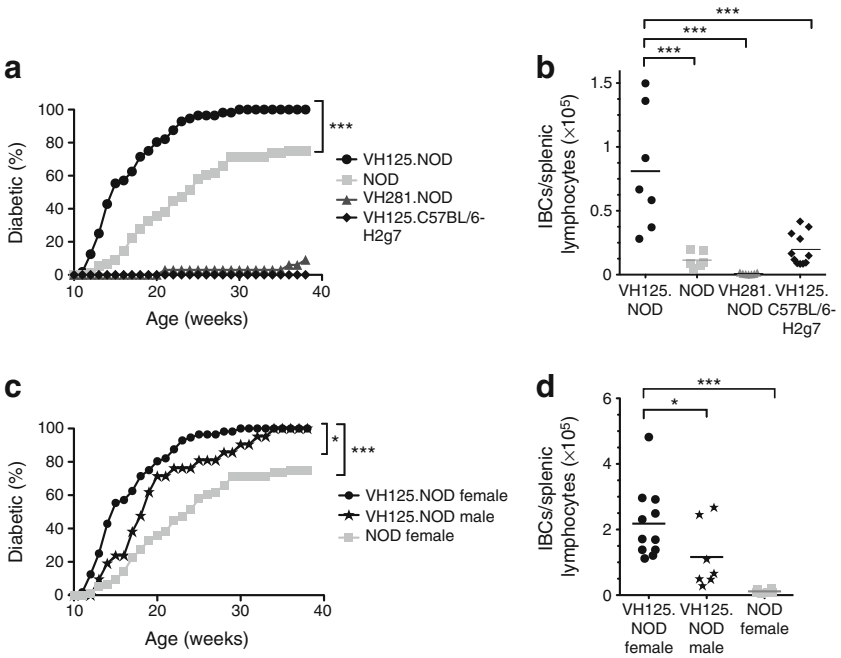

Fig. 2 BCR specificity for insulin contributes to development of diabetes in NOD mice. (**a**) Disease development in female VH125.NOD ($n = 56$), NOD ($n = 74$), VH281.NOD ($n = 31$) and VH125.C57BL/6-H2g7 ($n = 45$) mice based on weekly blood glucose monitoring from weaning until disease onset or 40 weeks of age. (**b**) Total splenic IBC numbers ($B220^+$) for 8- to 12-week-old female mice. (**c**) Male VH125.NOD ($n = 21$) were evaluated in the same manner as in (**a**). Black circles, female VH125.NOD mice; light grey squares, female NOD mice. (**d**) Total splenic IBC numbers ($B220^+$) for 10- to 20-week-old mice. The mean for each group is plotted as a horizontal line. Statistically significant differences in disease development were determined by logrank tests. Differences in the number of IBCs between the various strains were determined by unpaired Student's *t* tests; $*p < 0.05$, $***p < 0.001$

IBC frequency is directly correlated with penetrance and rate of onset of type 1 diabetes in NOD mice If IBCs play a limiting role in the development of type 1 diabetes [6], one would expect that disease development should correlate with IBC frequency. To explore this relationship, we analysed the rate of onset and penetrance of disease in mice that had differing frequencies of IBCs.

In VH125.NOD mice around 1–1.5% of splenic B cells bound insulin when not enriched (Fig. 1d), compared with around 20% when they were enriched (Fig. 1e). Similar to previous findings [6], all of these female mice developed disease by 30 weeks of age (Fig. 2a). In age-matched, non-transgenic female NOD mice, about one tenth the number of splenic IBCs was seen and disease onset was delayed, with 70% of mice being diabetic at 30 weeks (Fig. 2a). The IgM heavy chain VH281 differs from VH125 in that it lacks two amino acids in CDR2, and is not permissive for insulin binding, regardless of the paired light chain [6]. No IBCs were detectable in VH281.NOD mice, and less than 5% of female VH281.NOD mice developed type 1 diabetes (Figs 1d, 2a). The few that developed disease had lost allelic exclusion, as indicated by an expression of endogenous μ^b heavy chains (data not shown). Thus disease development may have been supported by cells that acquired insulin reactivity via endogenous Ig gene usage. Interestingly, despite having more peripheral IBCs than wild-type NOD mice, VH125.C57BL/6-H2g7 mice did not develop diabetes (Figs 1d, 2a). This suggests that these IBCs may be functionally silenced.

As shown in Fig. 2c, the female sex bias for the development of type 1 diabetes was maintained in the presence of the VH125 transgene. Although disease was observed in 100% of male VH125.NOD mice, the rate of development was statistically significantly lower than in females. The sex difference also correlated with varying frequency of splenic IBCs (Fig. 2d). Thus sex-based factors that affect disease probably also affect the frequency of IBCs.

Taken together, these results are consistent with the possibility that the rate and penetrance of type 1 diabetes in genetically predisposed mice are determined in part by the number of IBCs present, which could be an effect of sex.

VH125.NOD mice display defects in peripheral tolerance It has previously been shown that in VH125.NOD mice immature IBCs transition from the parenchyma to the sinusoids of the bone marrow and exit to the periphery of the immune system with no reduction in number, consistent with a defect in central tolerance [29]. We wanted to determine whether these mice also show a defect in peripheral tolerance.

During our studies, we identified two discrete IBC populations in both VH125.NOD and VH125.C57BL/6-H2g7 mice that distributed on distinct diagonals when analysed for IgM expression and insulin binding (Fig. 3a). The high IBC

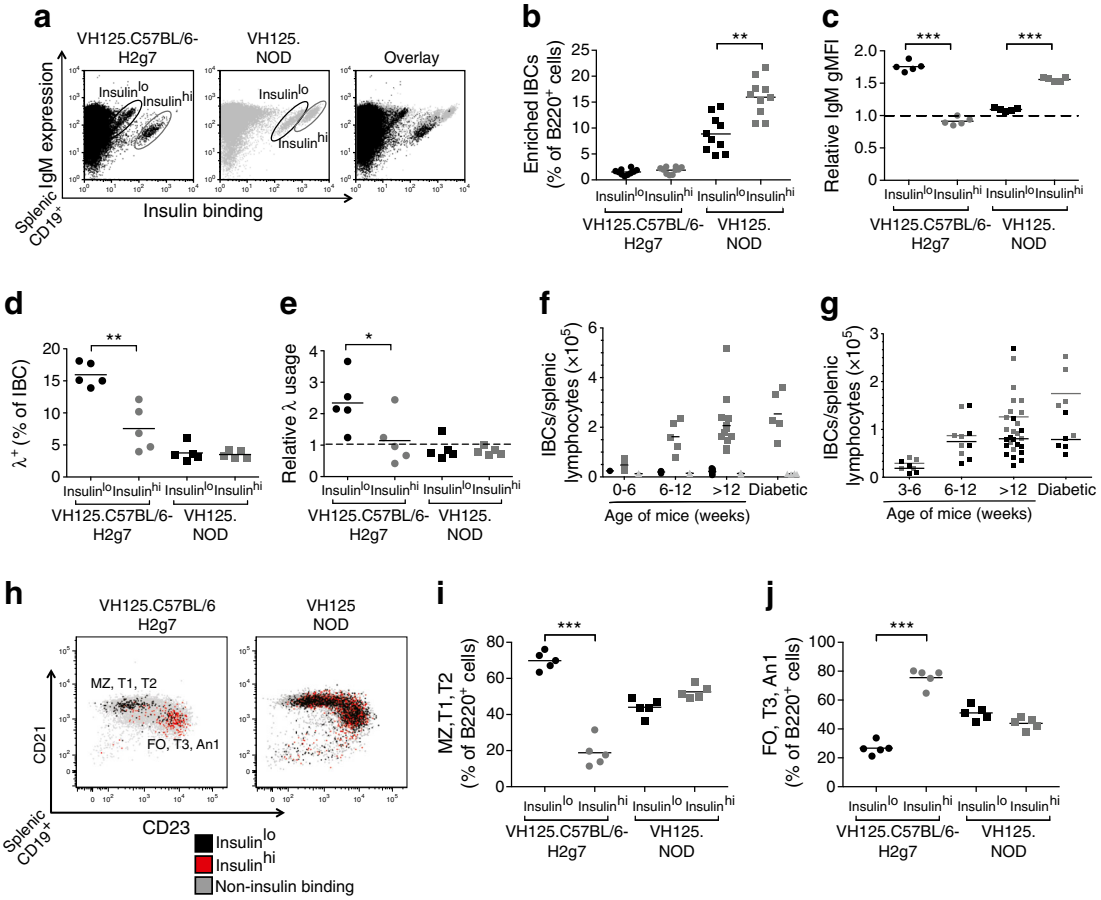

Fig. 3 Defective peripheral silencing of IBCs in NOD mice. (**a**) Representative cytograms of IgM expression vs insulin binding in VH125.C57BL/6-H2g7 and VH125.NOD mice. Staining reveals a low-affinity IBC population, designated Insulin^{lo} (black ovals), and a high-affinity IBC population, Insulin^{hi} (grey ovals), in VH125.C57BL/6-H2g7 mice. In VH125.NOD mice, both the Insulin^{lo} and Insulin^{hi} B cell populations had a high affinity for antigen. The two cytograms are overlaid for comparison of IgM levels and insulin reactivity. (**b**) Enriched IBCs as a percentage of B220^{+} cells for Insulin^{lo} and Insulin^{hi} B cells in VH125.C57BL/6-H2g7 and VH125.NOD mice. (**c**) Relative IgM expression (compared with non-IBCs) of Insulin^{lo} and Insulin^{hi} B cells in VH125.C57BL/6-H2g7 and VH125.NOD mice. (**d**, **e**) Percentage and relative usage of λ (compared with non-IBCs) of splenic λ-positive CD19^{+} B cells in the Insulin^{lo} and Insulin^{hi} B cell populations from the two strains. (**f**) Changes in the number of splenic IBCs with age and progression to type 1 diabetes in VH125.C57/B6-H2g7 (black circles), VH125.NOD (dark grey squares) and wild-type NOD mice (light grey triangles). (**g**) Changes in the number of Insulin^{lo} (black squares) and Insulin^{hi} (grey squares) splenic B cells in VH125.NOD mice with age and progression to type 1 diabetes. (**h**) Representative cytograms and splenic B cell subpopulation distribution of Insulin^{lo} (black), Insulin^{hi} (red) and non-IBC (light grey) cells in the spleen of 10-week-old VH125.C57BL/6-H2g7 and VH125.NOD mice. MZ, marginal zone; T1, transitional type 1; T2, transitional type 2, FO, follicular; T3, transitional type 3; An1, anergic. (**i**) MZ, T1 and T2 B cells are CD21^{hi} CD23^{lo}. (**j**) FO, T3 and An1 cells are CD21^{lo} CD23^{hi}. Results are representative of at least three experiments with at least three mice in each group. The mean for each group is shown as a horizontal line. $*p < 0.05$, $**p < 0.01$, $***p < 0.001$, Mann–Whitney *U* tests

population, designated Insulin^{hi}, was significantly enriched compared with the Insulin^{lo} population in VH125.NOD mice (Fig. 3b). Interestingly, in VH125.C57BL6-H2g7 mice, the Insulin^{lo} expressed higher levels of surface IgM than the right-shifted Insulin^{hi} population (Fig. 3a, c). This differed from the VH125.NOD mice, in which both the Insulin^{lo} and Insulin^{hi} B cell populations expressed high IgM levels compared with the non-IBCs (Fig. 3a, c). Based on our studies in humans, we suspect that the Insulin^{lo} B cell population in VH125.C57BL/6-H2g7 mice has sufficiently low insulin affinity that cells are ignorant of ambient insulin, despite being captured by the enrichment procedure [12]. On the other hand, the Insulin^{hi} B cell population in VH125.C57BL/6-H2g7 mice has sufficiently high affinity that cells are rendered anergic, as indicated by IgM downregulation compared with non-IBCs and the Insulin^{lo} population (Fig. 3c). Conversely, it appears that the Insulin^{hi} cells in VH125.NOD mice are not anergic since IgM levels remain high (Fig. 3c).

In order to further analyse the status of these cells, we explored their history of receptor editing by analysing the ratio of λ:κ BCR light chain usage, often used as a surrogate measure of receptor editing (Fig. 3d, e) [30]. In general, the frequency of λ^{+} cells was higher among IBCs from VH125.C57BL/6-H2g7 than VH125.NOD mice. It thus appears that fewer IBCs have

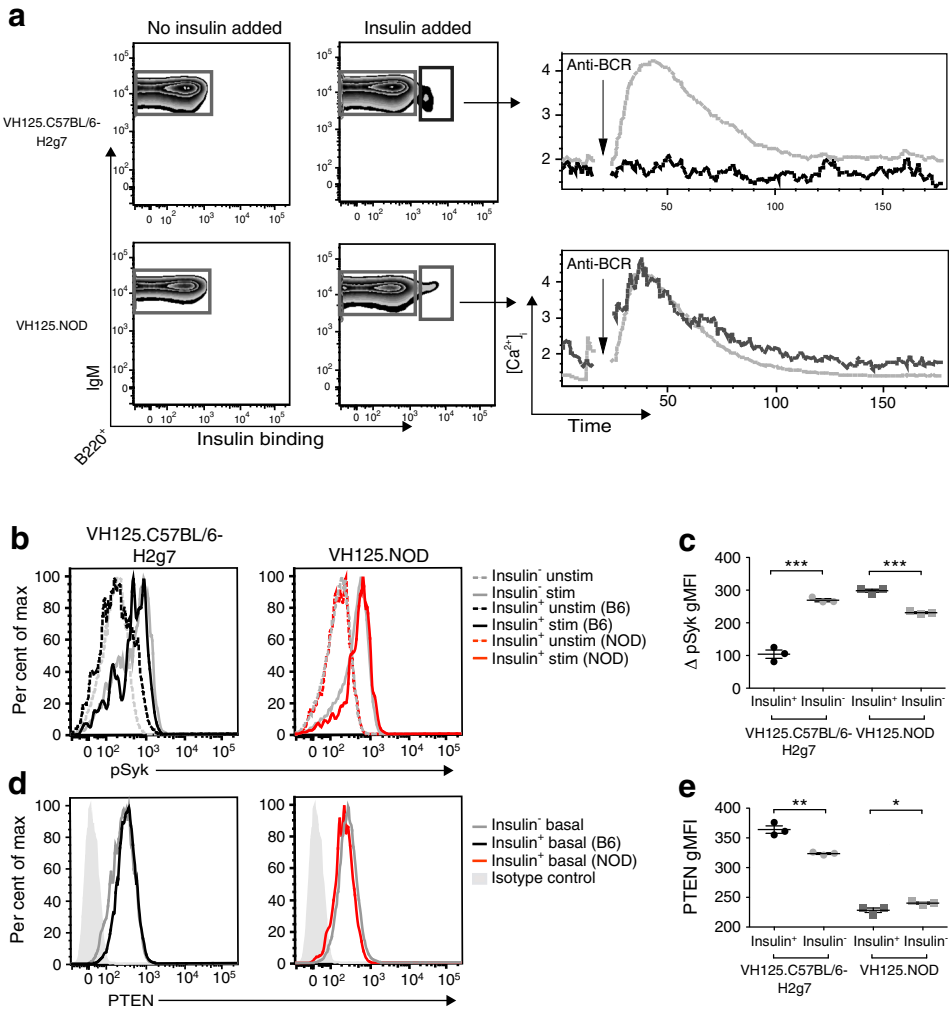

Fig. 4 IBCs in VH125.NOD are functionally responsive. (**a**) Gating strategy to identify IBCs in VH125.C57BL/6-H2g7 and VH125.NOD mice for assay of calcium mobilisation. Cytograms depicting gates when insulin is omitted are shown for comparison and to demonstrate the specificity of the binding. IBCs in VH125.C57BL/6-H2g7 mice are probably Insulin^{hi} due to decreased mIgM expression and do not show a mobilisation of intracellular calcium ($[Ca^{2+}]_i$) following stimulation (black line) compared with non-IBCs (light grey line), indicative of anergy. IBCs in VH125.NOD mice show increased mIgM expression and equal calcium mobilisation (dark grey line) compared with non-IBCs (light grey line), suggesting they are not anergic. (**b**) Representative histograms of pSyk before (dotted lines) and after (solid lines) stimulation in non-IBCs (Insulin$^-$) and IBCs (Insulin$^+$) from VH125.C57BL/6-H2g7 (B6) and VH125.NOD (NOD) mice. Gating on IBCs and non-IBCs is similar to that shown in Fig. 1b. Stim, stimulated; unstim, unstimulated. (**c**) Change in geometric MFI (gMFI) of phosphorylated Syk following stimulation in IBCs and non-IBCs in the two strains. (**d**) Representative basal PTEN levels in non-IBCs and IBCs from the two strains. Gating on IBCs and non-IBCs is similar to that shown in Fig. 1b. (**e**) Basal PTEN levels in IBCs vs non-IBCs in VH125.C57BL/6-H2g7 and VH125.NOD mice. Results are representative of at least three independent experiments with at least three mice per group. Results from the other two experiments demonstrated a greater than 70% decrease in calcium flux in IBCs from all VH125.C57BL/6-H2g7 mice assayed compared with IBCs in VH125.NOD mice. In the experiments not shown, the ΔgMFI of pSyk in IBCs from VH125.C57BL/6-H2g7 mice was on average (mean) 145 and 128 times less than that for Insulin$^-$ cells ($p < 0.01$ for both experiments), whereas the IBCs from VH125.NOD mice had a gMFI on average 43 and 65 times higher than that in non-IBCs ($p < 0.01$ and $p < 0.001$, respectively). Basal PTEN levels in IBCs from VH125.C57BL/6-H2g7 mice showed an average 30 and 62 times higher gMFI than non-IBCs ($p < 0.05$ and $p < 0.01$, respectively), whereas IBCs from VH125.NOD mice had on average a 22 and 37 times lower gMFI than non-IBCs (*$p < 0.05$ for both). For stimulation experiments, cells were stimulated with 5 μg/ml of F(ab′)$_2$ goat anti-mouse IgM. *$p < 0.05$, **$p < 0.01$, ***$p < 0.001$ determined by Mann–Whitney *U* test. Data in (**c**) and (**e**) are mean ± SEM

undergone receptor editing in NOD mice. Moreover, the Insulin^{lo} IBCs in the VH125.C57BL/6-H2g7 mice expressed significantly more λ light chains than their Insulin^{hi} counterparts (Fig. 3d, e). Again, we suggest that, in these cells, significant insulin autoreactivity has been edited away, so the cells become ignorant of their antigen.

Analysis of the relative number of IBCs in the periphery as a function of the age of the animal provided additional evidence of a difference in autoreactive B cells between the various genetic backgrounds (Fig. 3f). The total number of splenic IBCs in VH125.NOD mice increased nearly fourfold between weaning (around 0.5×10^5/spleen) and the onset of

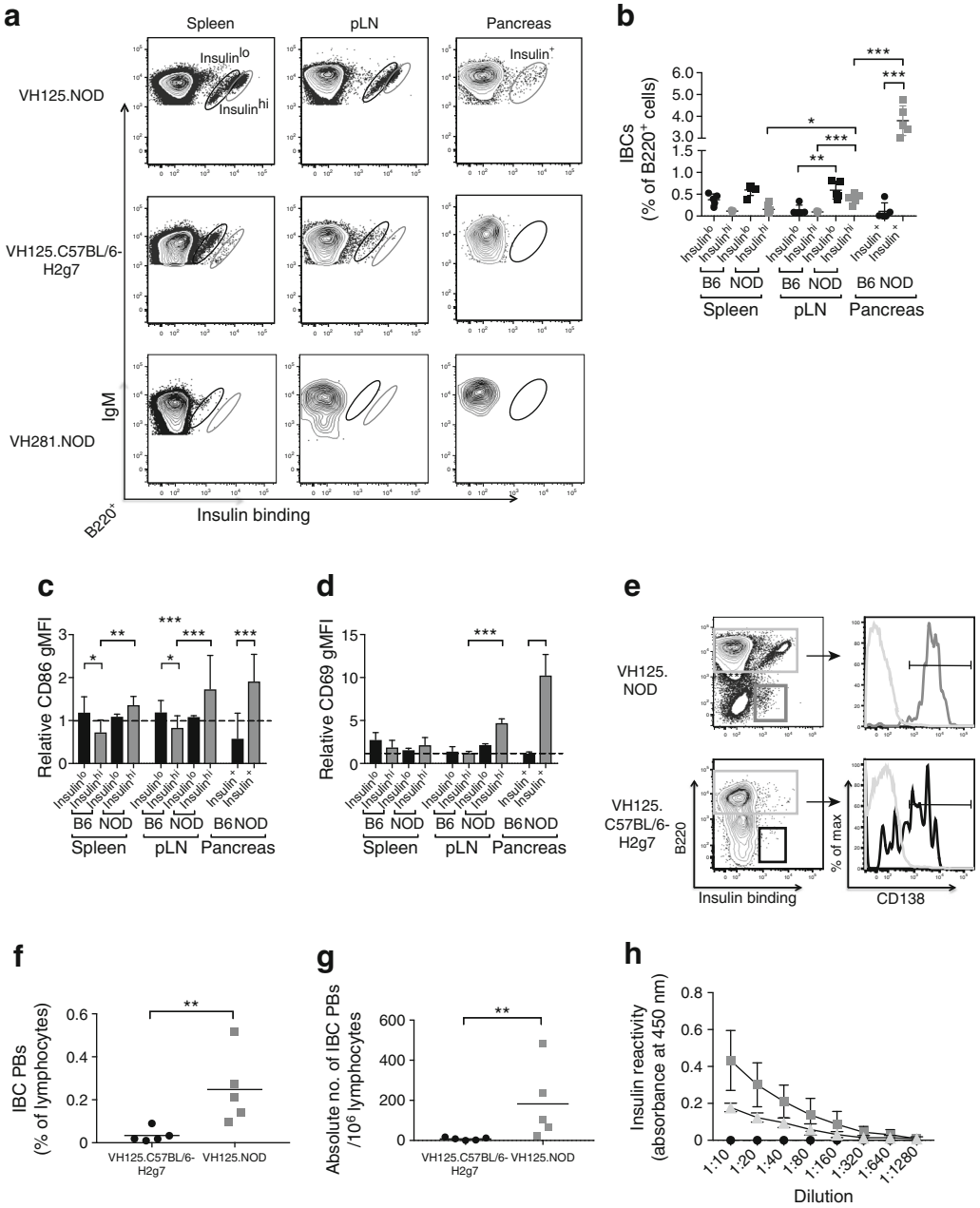

Fig. 5 IBCs in VH125.NOD mice accumulate in the pLNs and pancreas, express activation markers and produce autoantibodies. (**a**) Representative cytograms of Insulin^{lo}, Insulin^{hi} and Insulin^{+} B cells in the spleen, pLNs and pancreas from unenriched tissue samples. Staining from VH281.NOD mice is shown as a negative control for insulin binding. (**b**) IBCs as a percentage of B220^{+} B cells are compared for each organ in the two strains. IBCs accumulate in the pLNs and pancreas of VH125.NOD (NOD) but not VH125.C57BL/6-H2g7 (B6) mice. (**c**, **d**) Relative CD86 and CD69 geometric MFI (gMFI) of IBCs compared with non-IBCs in each organ is compared for the two strains. Insulin^{hi} B cells in VH125.NOD mice upregulate both activation markers. (**e**) Representative gating strategy for IBC plasmablasts (PBs) in the pLNs of both strains. (**f**) The percentage of IBC PBs is increased in the pLNs of VH125.NOD compared with VH125.C57BL/6-H2g7 mice. The percentage of IBC PBs was determined by multiplying the frequency of B220^{lo} IBC^{+} cells in the lymphocyte gate in the pLNs by the percentage that were also CD138^{+}. (**g**) The absolute number of IBC PBs is also increased in the pLNs of VH125.NOD compared with VH125.C57BL/6-H2g7 mice. (**h**) ELISA of serum demonstrating that IBCs in VH125.NOD (dark grey squares), but not VH125.C57BL/6-H2g7 (black circles) mice, probably produce anti-insulin antibodies, and are increased compared with wild-type NOD (light grey triangles) mice. Insulin reactivity in the serum of VH125.NOD mice was significantly elevated compared with VH125.C57BL/6-H2g7 mice ($p < 0.01$). All experiments used $n = 5$ female, non-diabetic, 8- to 12-week-old mice. Results are representative of at least three experiments with at least three mice per group. *$p < 0.05$, **$p < 0.01$, ***$p < 0.001$; Mann–Whitney U tests were used for all assays except ELISA, in which a one-way ANOVA with repeated measures was used

overt type 1 diabetes (around 2×10^5/spleen) (Fig. 3f), whereas no such accumulation of IBCs occurred in wild-type NOD and VH125.C57BL/6-H2g7 animals. The total number of splenic IBCs in VH125.C57BL/6-H2g7 mice remained low and constant regardless of age, consistent with a maintenance of peripheral tolerance.

To better understand their contribution to disease development, we assessed the relative numbers of B cells with high vs low insulin affinity as a function of age in the VH125.NOD mice (Fig. 3g). The Insulin^{lo} IBCs were present in spleen at the earliest time point examined (weaning) and increased in number until the B cell compartment matured, i.e. about 6 weeks of age. Whereas the frequency of low-affinity splenic IBCs remained relatively constant after 6 weeks of age, the frequency of Insulin^{hi} IBCs continued to increase until the onset of diabetes (Fig. 3g).

Next, we determined the distribution of Insulin^{lo} and Insulin^{hi} B cells in various splenic B cell subcompartments in the two strains. Insulin^{hi} B cells in the VH125.C57BL/6-H2g7 mice were CD21^{lo} and CD23^{hi} (Fig. 3h–j), consistent with the previously defined naturally occurring anergic An1 cells [28]. In contrast, VH125.C57BL/6-H2g7 Insulin^{lo} B cells were distributed in all major splenic B cell compartments, consistent with the possibility they are ignorant of ambient antigen. Importantly, both the Insulin^{hi} and Insulin^{lo} B cell populations in VH125.NOD mice had higher surface IgM levels (Fig. 3c), and occurred in all major splenic B cell populations (Fig. 3h–j), consistent with lack of anergy.

IBCs in VH125.NOD, but not VH125.C57BL/6-H2g7, mice were responsive to stimulation and had significantly decreased expression of PTEN To assess anergy we determined the responsiveness of IBC populations to BCR stimulation. To mark IBCs without stimulating them, we labelled cells with biotinylated insulin and detected them using fluorescent Fab anti-biotin (Fig. 4a). Of note, this method did not enable the resolution of Insulin^{hi} and Insulin^{lo} B cell populations based on antigen binding, probably due to decreased signal amplitude. However, because the IBCs in the VH125.C57BL/6-H2g7 mice had decreased IgM expression, we believe this method identifies Insulin^{hi} B cells when these markers are paired. Similarly, because IBCs in the VH125.NOD mice showed increased IgM expression, we believe that the approach captures at least the Insulin^{hi} B cells, if not also the Insulin^{lo} B cells (Fig. 4a).

When stimulated with F(ab′)$_2$ goat anti-IgM, VH125.C57BL/6-H2g7 IBCs failed to show a mobilisation of intracellular calcium (Fig. 4a), a classic indication of anergy. VH125.NOD IBCs responded well, mobilising calcium comparably to non-IBCs in NOD and C57BL/6-H2g7 mice (Fig. 4a). A similar relationship was seen in tyrosine phosphorylation of the BCR-proximal tyrosine kinase Syk. Although the shift was small, IBCs from VH125.C57BL/6-H2g7 mice showed significantly less induction of Syk phosphorylation than non-IBCs (Fig. 4b, c), demonstrating a dampened signalling response consistent with anergy. Of note, the decreased change in pSyk after stimulation was in part due to elevated basal pSyk in the IBCs (mean MFI 276) compared with the non-IBCs (mean MFI 164), presumably due to chronic antigen stimulation, which maintains anergy. IBCs from VH125.NOD mice showed enhanced pSyk following stimulation compared with non-IBCs (Fig. 4b, c), confirming they were not anergic.

Expression of PTEN is increased in anergic B cells in the MD4/ML5 transgenic mouse model and it is partially responsible for the hyporesponsiveness of anergic B cells [31, 32]. When we compared the expression of PTEN in IBCs vs non-IBCs, we found that IBCs from VH125.C57BL/6-H2g7 mice had significantly elevated levels of PTEN compared with non-IBCs (Fig. 4d, e). However, IBCs from VH125.NOD mice showed a significantly decreased expression of PTEN compared with non-IBCs (Fig. 4d, e), a finding consistent with the recent report of reduced PTEN expression in B cells from individuals with autoimmune systemic lupus erythematosus [33]. It should be noted that although the shifts are significant, they are small shifts in flow cytometric terms.

Taken together, these results demonstrate that IBCs in the VH125.C57BL/6-H2g7 mouse are functionally anergic, while those in VH125.NOD are not.

IBCs in VH125.NOD mice accumulate in pancreatic lymph nodes and pancreas prior to disease onset If IBCs in VH125.NOD mice have escaped tolerance and participate in disease, one might expect them to enter tissues rich in autoantigen and pertinent to the development of diabetes. Hence, we next compared the frequency of these cells in unenriched pancreatic lymph node (pLN) and pancreas samples to those in spleen samples in non-diabetic mice. As shown in Fig. 5a, b, we were able to detect both Insulin^{lo} and Insulin^{hi} B cells in the pLNs in VH125.NOD mice, but were only able to detect Insulin^{lo} IBCs, which we presume are immune-ignorant and do not participate in disease, in the pLNs in VH125.C57BL/6-H2g7 mice. Moreover, the frequency of IBCs, particularly due to an increase in the Insulin^{hi} B cells in the pLNs, significantly increased compared with the spleen in VH125.NOD mice, whereas the proportion of Insulin^{hi} B cells decreased, although not significantly, in the pLNs of VH125.C57BL/6-H2g7 compared with spleen (Fig. 5b). These results suggest that these cells are accumulating and/or expanding in the draining lymph nodes in NOD mice even prior to disease onset.

We rarely detected IBCs in the pancreas of VH125.C57BL/6-H2g7 mice and were unable to distinguish Insulin^{lo} from Insulin^{hi} cells in the VH125.NOD animals; we therefore refer to them as Insulin^{+} (Fig. 5a, b). It has been shown that the BCRs of IBCs in the pancreas are often coated with insulin, which may have inhibited our ability to discern the two populations [29]. Nonetheless, based on the cells we could detect, there was a significant increase in frequency in VH125.NOD

mice of IBCs in the pancreas compared with the pLNs or spleen, suggesting that high-affinity IBCs are entering the site of autoimmune attack prior to disease onset. On the other hand, no or few IBCs (or B cells; data not shown) could be detected in the pancreas of VH125.C57BL/6-H2g7 mice (Fig. 5a, b), suggesting that these cells are restricted to lymphoid tissues such as the spleen, and they are anergic.

IBCs in VH125.NOD mice show signs of activation prior to disease onset Hypothesising that high-affinity VH125.NOD IBCs that have broken tolerance and entered tissues rich in autoantigen may participate in disease through antigen presentation and/or autoantibody production, we next examined whether these cells exhibit markers of activation. We found that both the Insulin^{hi} and Insulin^{lo} splenic B cells in VH125.NOD mice have a slightly increased expression of CD86, whereas in C57BL/6-H2g7 the Insulin^{hi} B cells have a significantly lower expression of CD86 (Fig. 5c) compared with non-IBCs [19]. The Insulin^{hi} and Insulin^{+} B cells in the pLNs and pancreas of VH125.NOD mice showed significantly upregulated CD86 and CD69 compared with the Insulin^{lo} B cells and Insulin^{hi} B cells in the VH125.C57BL/6-H2g7 mice (Fig. 5c, d). These findings are consistent with an accumulation of Insulin^{hi}, but not Insulin^{lo}, B cells in the pLNs (and pancreas) of VH125.NOD mice. Taken together, IBCs accumulate in the pLN and pancreas in VH125.NOD, but not VH125.C57BL/6-H2g7, mice, and these cells show evidence of activation.

Next, we examined whether IBCs in the two strains give rise to plasmablasts. Although both the frequency and absolute number (Fig. 5f, g) of IBC plasmablasts in the pLNs were negligible in VH125.C57BL/6-H2g7 animals, the frequency and absolute number of IBC plasmablasts were significantly elevated in VH125.NOD mice (Fig. 5f, g). Furthermore, we were able to detect insulin-specific autoantibodies in VH125.NOD but not VH125.C57BL/6-H2g7 animals, and these were increased compared with wild-type NOD mice (Fig. 4h). Hence, these findings indicate that the IBCs in disease-prone VH125.NOD, but not disease-resistant VH125.C57BL/6-H2g7, mice accumulate in the pancreas and pLNs, where they become activated and probably produce autoantibodies prior to disease development.

Discussion

Previous studies have demonstrated a critical role for islet antigen-reactive B cells in the development of type 1 diabetes in the NOD mouse, and have implicated B cells in human type 1 diabetes. Studies in humans have further documented the occurrence of high-affinity IBCs in the peripheral blood of healthy individuals and shown that these cells leave the anergic compartment in blood prior to the development of type 1 diabetes [12]. Although the destination of these cells has not been fully elucidated, preliminary studies suggest that high-affinity IBCs in humans may relocate to the pLNs and pancreas and display an activated phenotype. This possibility is suggested by the histological detection of B cells in the pancreas, particularly in early-onset diabetes [34]. Due to the inherent limitations in studying this process in humans, we undertook the analysis in VH125.NOD mice and here report results that support the hypothesis and further suggest that IBCs become activated prior to arrest in the pancreas.

The results of this study provide new clarity regarding the status of IBCs in health and type 1 diabetes-prone settings. We demonstrate that, in disease-resistant settings, high-affinity IBCs can escape central tolerance, inhabiting the periphery where they are phenotypically and functionally anergic, similar to studies in healthy individuals [12]. However, previous studies have suggested that these B cells in the Tg125 mouse are also anergic in NOD animals, despite their requirement for disease [6, 15, 18]. This conundrum is clarified by the findings reported here that high-affinity IBCs lose anergy when they make up only a low percentage of the repertoire in NOD mice, avoiding the artefacts associated with using total-BCR-transgenic mice. Our studies demonstrate that IBCs in NOD mice are less efficiently eliminated by central tolerance mechanisms, occurring in the periphery at a seven- to eightfold higher frequency, progressively accumulate from birth in the spleens of these mice and then further accumulate in the pLNs and pancreas prior to disease onset. They occupy all major B cell compartments in the spleen and are not anergic, as indicated by high mIgM expression, a robust response to BCR stimulation and the upregulation of activation markers CD86 and CD69. The ability of high-affinity IBCs in the VH125.NOD mouse to upregulate CD86 suggests that these cells may participate in disease through antigen presentation to T cells, something that has already been shown in vitro despite claims they are anergic [18, 35].

In addition, our results are also novel in that IBCs from NOD mice showed normal calcium fluxes after addition of F(ab′)$_2$ anti-IgM, while B6 IBCs did not, consistent with an absence and presence of anergy, respectively. A previous study claimed, based on an a lack of calcium flux after stimulation with monomeric insulin, that IBCs in NOD mice were anergic [18]. However, a multitude of studies have shown that the induction of calcium responses by B cells requires crosslinking of BCRs, something that monomeric insulin is incapable of doing. This may explain why our results differ.

This study also raises an important question regarding whether and how the immune system perceives soluble monomeric autoantigens. There is general agreement that the induction of BCR signalling, like that of other immunoreceptor tyrosine-based activation motif (ITAM)-containing receptors, requires receptor aggregation. Classical studies have shown that antigen valence is critical for induction of B cell tolerance in vitro [36, 37]. It is likely that tolerance measured in these models reflects anergy. In view of this dependency and the

demonstrated requirement for chronic antigen exposure to induce and maintain anergy [38], it seems most likely that this response requires BCR aggregation. How could this occur in the VH125 model, where the autoantigen is monomeric? An obvious possibility is that B cells see insulin that is cell-associated by virtue of binding to the ubiquitous insulin receptor, CD220. However, the parent hybridoma, 125, antibody has been shown not to bind insulin that is associated with its receptor [22]. Another possibility is that these B cells recognise insulin that is associated with BCRs on other IBCs. This too is unlikely because the VH125 expressed on all B cells in this transgenic mouse would direct specificity of all IBCs to the same epitope regardless of light chain usage. Resolution of this question will clearly require more study.

In conclusion, comparative analysis of IBC status in disease-prone VH125.NOD and disease-resistant VH125.C57BL/6-H2g7 mice reveals how IBCs are likely to play a role in the development of type 1 diabetes, acting before the appearance of autoantibodies. This may provide a rationale for targeting these cells in the clinic to prevent type 1 diabetes, and provide essential tools for evaluating the efficacy and mode of action of candidate antigen-specific therapies.

Acknowledgements The authors would like to thank J. W. Thomas (Vanderbilt University, Nashville, TN, USA) for providing the VH125.NOD and VH125.C57BL/6 mice.

Data availability Data are available upon request from the corresponding author.

Funding This work was supported by grants from the National Institutes of Health (DP3DK110845, R21AI124488, R01AI124487, R01DK096492 and F30OD021477).

Duality of interest The authors declare that there is no duality of interest associated with this manuscript.

Contribution statement JCC designed the research and provided funding. MJS, RMH, TAP, AG, SK and JCC provided substantial contributions to conception and design, acquisition of data, and analysis and interpretation, as well as drafting the article and revising it critically; all authors have approved the version to be published. JCC is the guarantor of this work and, as such, had full access to all the data in the study and takes responsibility for the integrity of the data and the accuracy of the data analysis.

References

1. Serreze DV, Chapman HD, Varnum DS et al (1996) B lymphocytes are essential for the initiation of T cell-mediated autoimmune diabetes: analysis of a new "speed congenic" stock of NOD.Ig mu null mice. J Exp Med 184:2049–2053
2. Noorchashm H, Noorchashm N, Kern J, Rostami SY, Barker CF, Naji A (1997) B-cells are required for the initiation of insulitis and sialitis in nonobese diabetic mice. Diabetes 46:941–946
3. Pescovitz MD, Greenbaum CJ, Krause-Steinrauf H et al (2009) Rituximab, B-lymphocyte depletion, and preservation of beta-cell function. N Engl J Med 361:2143–2152
4. Hu CY, Rodriguez-Pinto D, Du W et al (2007) Treatment with CD20-specific antibody prevents and reverses autoimmune diabetes in mice. J Clin Invest 117:3857–3867
5. Xiu Y, Wong CP, Bouaziz JD et al (2008) B lymphocyte depletion by CD20 monoclonal antibody prevents diabetes in nonobese diabetic mice despite isotype-specific differences in Fc gamma R effector functions. J Immunol 180:2863–2875
6. Hulbert C, Riseili B, Rojas M, Thomas JW (2001) B cell specificity contributes to the outcome of diabetes in nonobese diabetic mice. J Immunol 167:5535–5538
7. Silveira PA, Johnson E, Chapman HD, Bui T, Tisch RM, Serreze DV (2002) The preferential ability of B lymphocytes to act as diabetogenic APC in NOD mice depends on expression of self-antigen-specific immunoglobulin receptors. Eur J Immunol 32:3657–3666
8. Silva DG, Daley SR, Hogan J et al (2011) Anti-islet autoantibodies trigger autoimmune diabetes in the presence of an increased frequency of islet-reactive CD4 T cells. Diabetes 60:2102–2111
9. Wong FS, Wen L, Tang M et al (2004) Investigation of the role of B-cells in type 1 diabetes in the NOD mouse. Diabetes 53:2581–2587
10. Marino E, Tan B, Binge L, Mackay CR, Grey ST (2012) B-cell cross-presentation of autologous antigen precipitates diabetes. Diabetes 61:2893–2905
11. Noorchashm H, Lieu YK, Noorchashm N et al (1999) I-Ag7-mediated antigen presentation by B lymphocytes is critical in overcoming a checkpoint in T cell tolerance to islet beta cells of nonobese diabetic mice. J Immunol 163:743–750
12. Smith MJ, Packard TA, O'Neill SK et al (2015) Loss of anergic B cells in prediabetic and new-onset type 1 diabetic patients. Diabetes 64:1703–1712
13. Smith MJ, Rihanek M, Coleman BM, Gottlieb PA, Sarapura VD, Cambier JC (2018) Activation of thyroid antigen-reactive B cells in recent onset autoimmune thyroid disease patients. J Autoimmun 89:82–89
14. Malkiel S, Jeganathan V, Wolfson S et al (2016) Checkpoints for autoreactive B cells in peripheral blood of lupus patients assessed by flow cytometry. Arthritis Rheum 68:2210–2220
15. Acevedo-Suarez CA, Hulbert C, Woodward EJ, Thomas JW (2005) Uncoupling of anergy from developmental arrest in anti-insulin B cells supports the development of autoimmune diabetes. J Immunol 174:827–833
16. Henry RA, Acevedo-Suarez CA, Thomas JW (2009) Functional silencing is initiated and maintained in immature anti-insulin B cells. J Immunol 182:3432–3439
17. Cambier JC, Gauld SB, Merrell KT, Vilen BJ (2007) B-cell anergy: from transgenic models to naturally occurring anergic B cells? Nat Rev Immunol 7:633–643
18. Kendall PL, Case JB, Sullivan AM et al (2013) Tolerant anti-insulin B cells are effective APCs. J Immunol 190:2519–2526
19. Gauld SB, Merrell KT, Cambier JC (2006) Silencing of autoreactive B cells by anergy: a fresh perspective. Curr Opin Immunol 18:292–297
20. Acevedo-Suarez CA, Kilkenny DM, Reich MB, Thomas JW (2006) Impaired intracellular calcium mobilization and NFATc1 availability in tolerant anti-insulin B cells. J Immunol 177:2234–2241
21. Thomas JW, Hulbert C (1996) Somatically mutated B cell pool provides precursors for insulin antibodies. J Immunol 157:763–771
22. Ewulonu UK, Nell LJ, Thomas JW (1990) VH and VL gene usage by murine IgG antibodies that bind autologous insulin. J Immunol 144:3091–3098
23. Packard TA, Smith MJ, Conrad FJ et al (2016) B cell receptor affinity for insulin dictates autoantigen acquisition and B cell functionality in autoimmune diabetes. J Clin Med 5:98

24. Baker RL, Bradley B, Wiles TA et al (2016) Cutting edge: nonobese diabetic mice deficient in chromogranin A are protected from autoimmune diabetes. J Immunol 196:39–43
25. Baker RL, Delong T, Barbour G, Bradley B, Nakayama M, Haskins K (2013) Cutting edge: CD4 T cells reactive to an islet amyloid polypeptide peptide accumulate in the pancreas and contribute to disease pathogenesis in nonobese diabetic mice. J Immunol 191: 3990–3994
26. Smith MJ, Packard TA, O'Neill SK et al (2017) Detection and enrichment of rare antigen-specific B cells for analysis of phenotype and function. J Vis Exp. https://doi.org/10.3791/55382
27. Goodnow CC, Crosbie J, Adelstein S et al (1988) Altered immunoglobulin expression and functional silencing of self-reactive B lymphocytes in transgenic mice. Nature 334:676–682
28. Merrell KT, Benschop RJ, Gauld S et al (2006) Identification of anergic B cells within a wild-type repertoire. Immunity 25:953–962
29. Henry-Bonami RA, Williams JM, Rachakonda AB, Karamali M, Kendall PL, Thomas JW (2013) B lymphocyte "original sin" in the bone marrow enhances islet autoreactivity in type 1 diabetes-prone nonobese diabetic mice. J Immunol 190:5992–6003
30. Mehr R, Shannon M, Litwin S (1999) Models for antigen receptor gene rearrangement. I. Biased receptor editing in B cells: implications for allelic exclusion. J Immunol 163:1793–1798
31. Browne CD, Del Nagro CJ, Cato MH, Dengler HS, Rickert RC (2009) Suppression of phosphatidylinositol 3,4,5-trisphosphate production is a key determinant of B cell anergy. Immunity 31: 749–760
32. Getahun A, Wemlinger SM, Rudra P, Santiago ML, van Dyk LF, Cambier JC (2017) Impaired B cell function during viral infections due to PTEN-mediated inhibition of the PI3K pathway. J Exp Med 214:931–941
33. Wu XN, Ye YX, Niu JW et al (2014) Defective PTEN regulation contributes to B cell hyperresponsiveness in systemic lupus erythematosus. Sci Transl Med 6:246ra299
34. Leete P, Willcox A, Krogvold L et al (2016) Differential insulitic profiles determine the extent of beta-cell destruction and the age at onset of type 1 diabetes. Diabetes 65:1362–1369
35. Henry RA, Kendall PL, Thomas JW (2012) Autoantigen-specific B-cell depletion overcomes failed immune tolerance in type 1 diabetes. Diabetes 61:2037–2044
36. Chiller JM, Weigle WO (1971) Cellular events during induction of immunologic unresponsiveness in adult mice. J Immunol 106: 1647–1653
37. Cambier JC, Kettman JR, Vitetta ES, Uhr JW (1976) Differential susceptibility of neonatal and adult murine spleen cells to in vitro induction of B-cell tolerance. J Exp Med 144:293–297
38. Gauld SB, Benschop RJ, Merrell KT, Cambier JC (2005) Maintenance of B cell anergy requires constant antigen receptor occupancy and signaling. Nat Immunol 6:1160–1167